

# Towards Viable Cosmological Solutions of Disformal Theories of Gravity

Jeremy Sakstein<sup>1,2,3</sup>

<sup>1</sup>*Department of Applied Mathematics and Theoretical Physics,  
Centre for Mathematical Sciences, Cambridge CB3 0WA, United Kingdom*

<sup>2</sup>*Institute of Cosmology and Gravitation, University of Portsmouth, Portsmouth PO1 3FX, UK*

<sup>3</sup>*Perimeter Institute for Theoretical Physics, 31 Caroline St. N, Waterloo, ON, N2L 6B9, Canada*

The late-time cosmological dynamics of disformal gravity are investigated using dynamical systems methods. It is shown that in the general case there are no stable attractors that screen fifth-forces locally and simultaneously describe a dark energy dominated universe. Furthermore, some attractors that are stable when the disformal coupling is absent are saddle points of the new system for certain parameter choices. When this is the case, the system evolves towards a dark energy dominated universe along a trajectory such that fifth-forces are unscreened and there is a singularity of the Jordan frame metric in the infinite future. This explains the natural pathology resistance observed numerically by several previous works. We identify a special parameter tuning such that there is a new fixed point that can match the presently observed dark energy density and equation of state whilst simultaneously satisfying local tests of gravity.

## I. INTRODUCTION

The observation of the acceleration of the cosmic expansion [1, 2] has prompted a renewed interest in modified theories of gravity as a potential driving mechanism. Amongst the plethora of candidate theories (see [3] for a review), those that contain screening mechanisms (see [4] for a review) have been particularly well-studied due to their ability to hide the additional or *fifth-* forces on solar system scales. Well-studied non-linear screening mechanisms—meaning that the local dynamics act to suppress fifth-forces—include the chameleon mechanism [5, 6] and similar [7, 8] as well as the Vainshtein mechanism [9]. These theories can be described by a conformal coupling of a scalar to matter through the metric [10]. Theories that contain a disformal coupling to matter have been studied in the context of dark matter and dark energy [11–18] but unlike chameleons, which have been well studied and constrained on small scales [19–24], the local behaviour of disformal theories has been relatively unstudied (although see [25, 26] for tests of TeVeS and a model that satisfies the Cassini bound on light bending by the Sun).

Recently, [18] have performed a thorough investigation into the local dynamics of the scalar. Non-relativistic objects inside a Friedmann-Robertson-Walker (FRW) universe will source a field profile such that the fifth-force is  $F_5 = 2Q^2 F_N - F_N$  is the Newtonian force—where the local scalar charge  $Q$  depends on the conformal coupling, the disformal parameters and the first and second time-derivatives of the cosmological field. There, it was argued that there are no non-linear screening mechanisms beyond those mentioned above. It was shown, however, that when the conformal coupling is absent [27] these theories screen linearly—by which we mean the local scalar charge is suppressed on all scales through the cosmological dynamics and not the local ones—whenever the cosmological dynamics are such that the field is slowly rolling.

The aim of this work is to investigate more general

models where the conformal factor is non-zero and see whether one can find models that can drive the cosmic acceleration at late times whilst simultaneously suppressing the local scalar charge. We will do this using dynamical systems techniques. These are powerful tools to classify the late-time behaviour of non-linear systems despite the lack of analytic solutions. Their power lies in their ability to classify all solutions of the system in terms of a few fixed points independently of the initial conditions. Without them, one would be reduced to solving the problem numerically for all possible parameters and initial conditions, a problem that is clearly intractable. Since the relevant cosmological parameters have well-defined values at these points, one can know the final state the universe will evolve to. Dynamical systems methods have previously been used in the study of dark energy models in the form of quintessence [28] and conformally coupled theories [29] (see [30] for a review). There, they find dark energy dominated solutions by looking for points where the density parameter and equation of state is close to the observed values [31]. Here, we will do the same for the disformal system, examining the local scalar charge as well in order to classify the linear screening. Unlike the simple cases mentioned above, the disformal system requires use of the centre manifold technique, which is necessary whenever different directions in phase space evolve on different time-scales. Interestingly, we will see that some of the attractors of the conformal system are saddle points of the disformal system and the evolution can be very different at late times.

These theories have potential instabilities since the determinant of the Jordan frame metric can become singular. Several authors [13, 14, 16] have observed numerically that solutions tend to slow down to avoid this and have dubbed this phenomena a *natural resistance to pathology*. Using the techniques described above, we will show that any singularity is only reached in an infinite amount of time, thereby explaining this phenomena.

Since portions of this paper are technical, we state our main results unambiguously below:

- The phase space is three-dimensional, in contrast to the purely conformal case. There are no new dark energy dominated solutions and those present in the purely conformal case do not screen linearly.
- There are parameter choices where the purely conformal fixed points are saddle points. In this case, the system ultimately evolves towards a dark energy dominated solution where the determinant of the Jordan frame metric is singular and there are large unscreened fifth forces.
- There is a special tuning in parameter space where the dimension of the phase space is reduced to two. In this case there is a new stable attractor where the scalar charge is identically zero. Furthermore, by choosing the model parameters correctly one can reproduce the present dark energy density parameter and equation of state.

This paper is organised as follows: The theory is introduced in section II. Section III constitutes the main body of this work. There it is shown that there are no stable dark energy dominated solutions that simultaneously have zero local scalar charge. Furthermore, we show that the singularity in the Jordan frame metric is only reached in the infinite future. In section IV we examine the special parameter choices such that the phase space is two-dimensional and find a new fixed point that both screens and can reproduce the observed dark energy parameters. We conclude in section V. A brief introduction to dynamical systems including centre manifold techniques is provided in appendix A for the unfamiliar reader.

## II. DISFORMAL THEORIES OF GRAVITY

Disformal theories of gravity are described by the following action:

$$S = M_{\text{pl}}^2 \int d^4x \sqrt{-g} \left[ \frac{R}{2} + X - V(\phi) \right] + S_{\text{m}}[\tilde{g}; \Psi_i], \quad (1)$$

where the various matter fields  $\Psi_i$  are coupled to the Jordan frame metric

$$\tilde{g}_{\mu\nu} = A^2(\phi) \left( g_{\mu\nu} + \frac{B^2(\phi)}{\Lambda^2} \partial_\mu \phi \partial_\nu \phi \right), \quad (2)$$

and  $X \equiv -1/2 \nabla_\mu \phi \nabla^\mu \phi$ .  $g_{\mu\nu}$  is the Einstein frame metric.  $A$  and  $B$  are known as the *conformal* and *disformal* factors respectively and we define the following quantities[32]

$$\alpha(\phi) \equiv \frac{d \ln A(\phi)}{d\phi} \quad \text{and} \quad \gamma(\phi) \equiv \frac{d \ln B(\phi)}{d\phi}. \quad (3)$$

The determinants of the two metrics are related by (see [16], appendix A)

$$\frac{\sqrt{-\tilde{g}}}{\sqrt{-g}} = A^4 \sqrt{1 - \frac{2B^2 X}{\Lambda^2}}. \quad (4)$$

Note that it is possible for the right hand side to become zero so that the metric is singular, which is a potential problem for the theory. Cosmologically, several authors [13, 14, 16] have numerically found a *natural resistance to pathology* in the solutions where the cosmological time-evolution of the field slows down at late times and the singularity is avoided. We will address this issue later and show that certain models can evolve towards the metric singularity but only in an infinite time, thereby explaining the numerical observations of this pathology resistance.

The background cosmology (in coordinate time) is determined by the Friedmann equations

$$3H^2 = 8\pi G \rho_{\text{m}} + \frac{\dot{\phi}_\infty^2}{2} + V(\phi_\infty) \quad (5)$$

$$\dot{H} = -4\pi G \rho_{\text{m}} - \frac{\dot{\phi}_\infty^2}{2} \quad (6)$$

coupled to the equation of motion for the scalar and the matter density:

$$\ddot{\phi}_\infty + 3H\dot{\phi}_\infty + V(\phi_\infty)_{,\phi} = -Q_0 \quad \text{and} \quad (7)$$

$$\dot{\rho}_{\text{m}} + 3H\rho_{\text{m}} = Q_0\dot{\phi}_\infty \quad (8)$$

where

$$Q_0 = 8\pi G \rho_{\text{m}} \frac{\alpha + \frac{B^2}{\Lambda^2} ([\gamma - \alpha] \dot{\phi}_\infty^2 - 3H\dot{\phi}_\infty - V_{,\phi})}{1 + \frac{B^2}{\Lambda^2} (8\pi G \rho_{\text{m}} - \dot{\phi}_\infty^2)}, \quad (9)$$

and  $\rho = -T_{\text{m}}$  with  $T_{\text{m}}$  the trace of the Einstein frame energy-momentum tensor. Note that since the scalar is non-minimally coupled to matter the energy-momentum tensor is not covariantly conserved in this frame, which leads to the modified continuity equation (8). We do not include radiation or other particle species in this work since we are interested in the late-time behaviour of the system where all of these components are sub-dominant.

In [18], it was shown that when expanded around an FRW background, the fifth-force arising in these theories is

$$F_5 = 2Q^2 F_{\text{N}}, \quad (10)$$

where  $F_{\text{N}}$  is the Newtonian force and the local scalar charge  $Q$  is

$$Q \equiv \alpha + \frac{B^2}{\Lambda^2} (\ddot{\phi}_\infty + \dot{\phi}_\infty^2 [\gamma - \alpha]), \quad (11)$$

where  $\phi_\infty$  is the cosmological (homogeneous) component of the field. In [18], we examined models where  $\alpha(\phi) = 0$  and argued that any model where the scalar potential has a minimum can naturally screen fifth forces because at late-times, when the field is slowly-rolling,  $Q \approx 0$ . In this work, we wish to address the more general question: can we find models with  $\alpha \neq 0$  where the scalar charge is identically zero at late times and the universe is dark

energy dominated? In order to answer this, one must use dynamical systems techniques since this allows one to explore the entire solution space of the theory without numerically solving each model with every possible set of initial conditions.

### III. DYNAMICAL SYSTEMS ANALYSIS

#### A. Phase Space Construction

Dynamical systems have been used in cosmology (see [30] and references therein) to examine the late time behaviour of quintessence [28] and conformally coupled dark energy [29][33]. Here, we will extend the formalism to disformally coupled dark energy. A brief introduction to the general techniques is given in appendix A for the unfamiliar reader. We begin by introducing the new

variables

$$\begin{aligned} x &\equiv \frac{\phi'_\infty}{\sqrt{6}}, \quad y \equiv \frac{\sqrt{V}}{\sqrt{3}H}, \\ \lambda &\equiv -\frac{V_{,\phi}}{V}, \quad z \equiv \frac{BH}{\Lambda}, \end{aligned} \quad (12)$$

where we have changed from coordinate time  $t$  to  $N \equiv \ln a(t)$  and use a prime to denote derivatives with respect to  $N$ . In order to focus on the simplest case, we take  $\lambda$ ,  $\alpha$  and  $\gamma$  to be constant so that

$$V(\phi) = m_0^2 e^{-\lambda\phi}, \quad A(\phi) = e^{\alpha\phi} \quad \text{and} \quad B(\phi) = e^{\gamma\phi}, \quad (13)$$

where  $m_0$  is a mass scale associated with the scalar potential. Note that this is the coupled dark energy model of [29] extended to include an exponential disformal coupling. Such a model has previously been studied by [16] with  $\alpha = 0$  and so this is a generalisation of their model to arbitrary conformal couplings. One should note that whereas this model makes a specific choice for the functional forms of the free functions, one can think of the fixed points found using this system as instantaneous fixed points for more complicated models. Written in these variables, the Friedmann-scalar field system can be written in first-order autonomous form:

$$\begin{aligned} \frac{dx}{dN} &= -3x + \frac{3}{2}x(1+x^2-y^2) + \sqrt{\frac{3}{2}}y^2\lambda \\ &+ \frac{\sqrt{\frac{3}{2}}(x^2+y^2-1)(\alpha+3z^2(2x^2(\gamma-\alpha)-\sqrt{6}x+y^2\lambda))}{1+3(1-3x^2-y^2)z^2}, \end{aligned} \quad (14)$$

$$\frac{dy}{dN} = \frac{3}{2}y(1+x^2-y^2) - \sqrt{\frac{3}{2}}xy\lambda \quad \text{and} \quad (15)$$

$$\frac{dz}{dN} = \sqrt{6}\gamma xz - \frac{3}{2}z(x^2-y^2+1). \quad (16)$$

These are to be supplemented with the Friedmann constraint

$$x^2 + y^2 + \Omega_m = 1, \quad (17)$$

where  $\Omega_m \equiv 8\pi G\rho_m/3H^2$ . This system is then three-dimensional. In terms of the variables  $\{\phi, a(t), \Omega_m\}$  we have a first-order equation for  $\Omega_m$  and second-order equations for  $\phi$  and  $a(t)$  implying that we have a five-dimensional phase space. Changing to the variables  $\{x, y, z\}$  there are three coupled first-order equations including the constants  $\{\lambda, \alpha, \gamma\}$ . The density parameter  $\Omega_m$  is eliminated using the Friedmann constraint and the choice of time coordinate  $N$  allows us to remove any dependence on  $a(t)$  so that  $x$ ,  $y$  and  $z$  are the only dynamical degrees of freedom. This is to be contrasted with the conformally coupled case where the phase space is

two-dimensional. This is because choosing  $\lambda$  and  $\alpha$  to be constant removes any dependence on  $\phi$  in the equations for  $x$  and  $y$  whereas  $B(\phi)$  remains in  $Q_0$  even when  $\gamma$  is constant. Note also that  $\gamma = 0$  does not reduce the dimensionality of the phase space because in this case  $z$  depends on  $H$ , which cannot be eliminated in terms of  $x$  and  $y$  only and so the case where  $B$  is constant is included in this analysis. On the other hand, when  $\gamma = \lambda/2$  we have the relation

$$zy = \frac{m_0}{\sqrt{3}\Lambda} \quad (18)$$

and so one may eliminate  $z$  in terms of  $y$  or vice versa. Therefore,  $\gamma = 2\lambda$  is a special hyperplane in parameter space[34] where the dimensionality of the phase space is reduced to two. This requires a separate analysis and so we will first treat the general three-dimensional phase

space dynamics and return to this later.

Next, one can express some useful quantities in terms of these variables:

$$\Omega_\phi = \frac{\dot{\phi}_\infty^2}{6H^2} + \frac{V(\phi)}{3H^2} = x^2 + y^2, \quad (19)$$

$$\omega_\phi = \frac{\dot{\phi}_\infty^2 - 2V}{\dot{\phi}_\infty^2 + 2V} = \frac{x^2 - y^2}{x^2 + y^2}, \quad (20)$$

$$D \equiv \frac{2B^2 X}{\Lambda^2} = 6x^2 z^2 \quad \text{and} \quad (21)$$

$$Q = \alpha + z^2 \left[ \sqrt{6}x + 6x^2(\gamma - \alpha) + 3\sqrt{\frac{3}{2}}x(y^2 - x^2 - 1) \right]. \quad (22)$$

$\Omega_\phi \sim 1$  corresponds to a dark energy dominated solution,  $Q = 0$  corresponds to the absence of any fifth-forces on small scales and  $D = 1$  signifies a singularity in the Jordan frame metric. The problem of finding dark energy dominated accelerating solutions where fifth-forces are absent is then reduced to finding stable fixed points of the autonomous system where  $\Omega_\phi$  and  $\omega_\phi$  are compatible with current dark energy observations and  $Q = 0$ .

### B. Fixed Points

Before studying the new system (14)–(16), it is worth recalling some useful properties of the equivalent system when only a conformal coupling is present, which corresponds to  $z = 0$ . This was studied by [29] (see also [30]). There are two stable fixed points:

- **Dark energy dominated fixed point:** This has  $\Omega_\phi = 1$  and  $\omega_\phi = -1 + \lambda^2/3$ . It exists whenever  $\lambda < \sqrt{6}$  and is stable whenever  $\lambda < (\sqrt{\alpha^2 + 12} - \alpha)/2$ .
- **Variable fixed point:** This may or may not give dark energy domination depending on the choice of parameters, although solutions which match the current observations suffer from the lack of a matter dominated era, at least when  $\alpha$  and  $\lambda$  are constant [35]. It is always stable but only exists when the dark energy dominated solution is unstable and is hence the only stable fixed point when  $\lambda > \sqrt{6}$ . There is a critical value of  $\alpha$  below which it is a stable node and above which it is a stable spiral.

In the case of a purely conformal coupling, the phase space is a semi-circle in the  $x$ – $y$  plane (we do not consider  $V(\phi) < 0$ ). Since  $z > 0$  ( $B > 0$  for stability reasons, see [16]) the phase-space of the disformal system is an infinite semi-circular prism restricted to the upper half of the  $z$  plane ( $z > 0$ ). This parametrisation could be problematic because  $z$  can potentially reach  $\infty$  and so there may be fixed points at infinity. Indeed, this is the case but we will analyse the fixed points of the system (14)–(16) first in order to make contact with the purely conformal case. Setting equations (14)–(16) equal to zero, we find

the fixed points given in table I. The cosmological relevant parameters are given in table II. Points (1)–(5) are the fixed points found by [29] for the purely conformal case, they have  $z = 0$  so that all disformal effects are absent[36]. Note also that these points have  $Q = \alpha$  and hence lead to large unscreened fifth-forces on all scales unless one tunes this to very small values. Since  $D = 0$  at these points the Jordan frame metric is non-singular at late times.

The new points are (6) and (7). These points have  $Q = 0$  identically and hence one would expect any fifth-forces to be small as one approaches these points. Unfortunately, these points behave as a stiff fluid ( $\omega_\phi = 1$ ) and so cannot describe a dark energy dominated universe. Furthermore, point (7) is unphysical except for the special point  $\gamma = \sqrt{3}/2$ ; when  $\gamma > \sqrt{3}/2$  one has  $\Omega_\phi > 1$  and the point lies outside the physical state space.

Since the dimension of the phase space is increased from the purely conformal case, the stability of the fixed points is altered; there are now three eigenvalues instead of two. In particular, whereas the purely conformal fixed points ((1)–(5)) do not depend on  $\gamma$ , their stability does. The eigenvalues,  $e_{1,2,3}$  for each fixed point are given in appendix B. One may check that there are choices of the parameters  $\alpha$ ,  $\gamma$  and  $\lambda$  where none of these fixed points are stable. Indeed, one may check that when  $\alpha = 5$ ,  $\gamma = 4$  and  $\lambda = 6$ , all of the fixed points are either unstable or saddle points. The trajectory in the  $x$ – $y$  plane of solutions with  $H_0/\Lambda = 10^{-2}$  and  $10^{-3}$  and initial conditions  $\phi_0 = -1$  and  $\phi'_0 = 0$  is shown in figure 1. Furthermore, we show the evolution of  $(1 - D)$  in figure 2. One can see that in each case, the system spends a long time near the saddle point before moving towards  $x = 0$ ,  $y = 1$ . Along this trajectory,  $(1 - D)$  approaches zero so that the universe is tending to a state where the Jordan frame metric is singular. Furthermore, one can see that this behaviour is independent of the choice of  $\Lambda$  and one can check that it is not affected by the initial conditions either. This suggests that the system has a common late-time behaviour not captured by the fixed-point analysis above. The next subsection is devoted to understanding this.

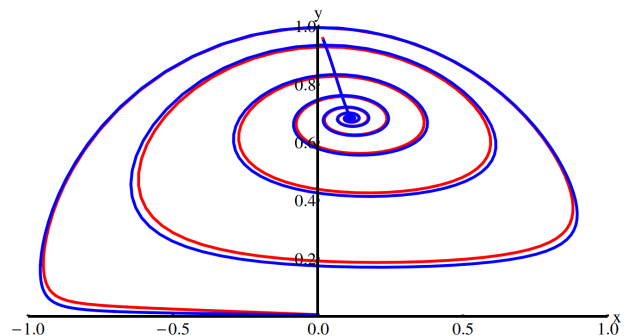
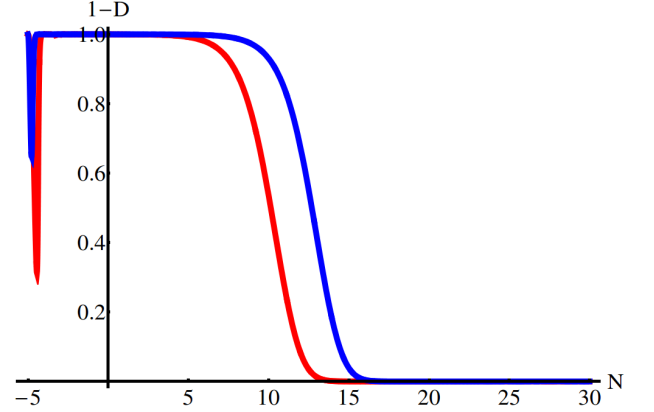


FIG. 1. The trajectories in the  $x$ – $y$  plane for  $\alpha = 5$ ,  $\gamma = 4$  and  $\lambda = 6$  with initial conditions  $\phi_0 = -1$  and  $\phi'_0 = 0$ . The red track corresponds to  $H_0/\Lambda = 10^{-2}$  and the blue track to  $H_0/\Lambda = 10^{-3}$ .

Name	$x$	$y$	$z$	Existence
(1)	$-\sqrt{\frac{2}{3}}\alpha$	0	0	$\alpha < \sqrt{3/2}$
(2)	-1	0	0	All
(3)	1	0	0	All
(4)	$\frac{\lambda}{\sqrt{6}}$	$\sqrt{1 - \frac{\lambda^2}{6}}$	0	$\lambda < \sqrt{6}$
(5)	$\frac{\sqrt{\frac{3}{2}}}{\alpha + \lambda}$	$\frac{\sqrt{3 + 2\alpha(\alpha + \lambda)}}{\sqrt{2(\alpha + \lambda)}}$	0	$\alpha > 3/\lambda - \lambda$
(6)	$\sqrt{\frac{2}{3}\gamma - \sqrt{\frac{2}{3}\gamma^2 - 1}}$	0	$\frac{1}{3}\sqrt{4\gamma^2 + \gamma\sqrt{4\gamma^2 - 6} - \frac{3}{2}}$	$\gamma > \sqrt{3/2}$
(7)	$\sqrt{\frac{2}{3}\gamma + \sqrt{\frac{2}{3}\gamma^2 - 1}}$	0	$\frac{1}{3}\sqrt{4\gamma^2 - \gamma\sqrt{4\gamma^2 - 6} - \frac{3}{2}}$	$\gamma = \sqrt{3/2}$

TABLE I. The fixed points of the system (14)–(16) with  $\gamma \neq \lambda/2$ .

Name	$Q$	$\Omega_\phi$	$\omega_\phi$	$D$
(1)	$\alpha$	1	1	0
(2)	$\alpha$	1	1	0
(3)	$\alpha$	$\frac{2\alpha^2}{3}$	1	0
(4)	$\alpha$	1	$-1 + \frac{\lambda^2}{3}$	0
(5)	$\alpha$	$\frac{3 + \alpha(\alpha + \lambda)}{(\alpha + \lambda)^2}$	$-1 + \frac{3}{3 + \alpha(\alpha + \lambda)}$	0
(6)	0	$\frac{1}{3} \left( \sqrt{-3 + 2\gamma^2} - \sqrt{2}\gamma \right)^2$	1	1
(7)	0	$\frac{1}{3} \left( \sqrt{-3 + 2\gamma^2} + \sqrt{2}\gamma \right)^2$	1	1

TABLE II. The cosmological quantities at the fixed points of the system (14)–(16) with  $\gamma \neq \lambda/2$ .FIG. 2.  $1 - D$  as a function of  $N$  for the models described in figure 1.

### C. Fixed Points at Infinity

Numerically, one finds that a continued integration of the system to later times pushes  $x$  closer to 0,  $y$  closer to 1 and  $z$  to increasingly larger values. This suggests that the behaviour may be due to fixed points at  $z = \infty$  and so we investigate these by compactifying the phase space. Defining

$$Z \equiv \frac{z}{z + 1} \quad (23)$$

so that  $0 \leq Z \leq 1$  we can map the points at  $z = \infty$  to  $Z = 1$  whilst  $z = 0$  corresponds to  $Z = 0$ . The phase space in these coordinates is then the finite semi-circular prism. In these coordinates, the system is described by the three first-order equations

$$\frac{dx}{dN} = -3x + \sqrt{\frac{3}{2}}\lambda y^2 + \frac{3}{2}x(x^2 - y^2 + 1) + \sqrt{\frac{3}{2}} \frac{(x^2 + y^2 - 1)(6x^2 Z^2(\alpha - \gamma) + 3\sqrt{6}xZ^2 - 3\lambda y^2 Z^2 - \alpha(Z - 1)^2)}{Z^2(9x^2 + 3y^2 - 4) + 2Z - 1}, \quad (24)$$

$$\frac{dy}{dN} = \frac{3}{2}y(1 + x^2 - y^2) - \sqrt{\frac{3}{2}}xy\lambda \quad \text{and} \quad (25)$$

$$\frac{dZ}{dN} = \frac{1}{2}(Z - 1)Z(3x^2 - 2\sqrt{6}\gamma x - 3y^2 + 3). \quad (26)$$

In addition to the fixed points found above, one finds the fixed points given in table III[37]. The cosmological parameters at each point are shown in table IV. We have omitted point (11) since this is discussed in detail in the next section. The eigenvalues are listed in appendix A 2 but here we note that the eigenvalues for point (11) are

$$e_1 = -3, \quad e_2 = 0 \quad \text{and} \quad e_3 = 0. \quad (27)$$

### 1. Centre Manifold Analysis

The two zero eigenvalues indicate that a linear analysis is not sufficient to determine the stability of the system near this fixed point. In order to do this, one must perform a centre manifold analysis. This has been used in cosmological systems previously (see [38] for a recent application to  $m^2\phi^2$  potentials and references therein for further examples) and we give a full account for the unfamiliar reader in appendix A 2. For simplicity, we move the point to the origin by making the change of variables:

$$Z = W + 1 \quad \text{and} \quad (28)$$

$$y = Y + 1. \quad (29)$$

We will not give the new first-order system here but for completeness it is given in appendix C. This change of variables does not change the eigenvalues but does change the eigenvectors, which, in this basis, are

$$\vec{e}_1 = \begin{pmatrix} 0 \\ 1 \\ 0 \end{pmatrix}, \quad \vec{e}_2 = \begin{pmatrix} 0 \\ 0 \\ 1 \end{pmatrix} \quad \text{and} \quad \vec{e}_3 = \begin{pmatrix} -\frac{\sqrt{6}}{\lambda} \\ 1 \\ 0 \end{pmatrix}, \quad (30)$$

where the first is an eigenvalue  $-3$  vector and the final two are zero-eigenvectors. This means that for any initial configuration sufficiently close to the fixed point, the trajectory along the  $\vec{e}_1$  direction will rapidly tend to its fixed point value whereas the trajectory in the plane described by  $\vec{e}_{1,2}$ —the centre manifold—will evolve on a slower time-scale. The essence of the centre manifold technique is to find the new variable along the  $\vec{e}_1$  direction and assume that its evolution equation is already

minimised. One can then solve this to obtain an algebraic expression for this variable in terms of those parametrising the centre manifold. The equations for the other two variables—the *centre variables*—then describe the dynamics in the centre manifold at late times. One has then reduced the dimension of the phase space to that of the centre manifold. Writing

$$\begin{pmatrix} x \\ Y \\ W \end{pmatrix} = \sum_i A_i \vec{e}_i, \quad (31)$$

one finds

$$\begin{pmatrix} x \\ Y \\ W \end{pmatrix} = \begin{pmatrix} -\frac{\sqrt{6}}{\lambda} A_3 \\ A_1 + A_3 \\ A_2 \end{pmatrix}, \quad (32)$$

from which we find

$$\begin{pmatrix} A_1 \\ A_2 \\ A_3 \end{pmatrix} = \begin{pmatrix} Y + \frac{\lambda}{\sqrt{6}}x \\ W \\ -\frac{\lambda}{\sqrt{6}}x \end{pmatrix}. \quad (33)$$

Setting  $A'_1 = 0$  i.e. the variable along  $\vec{e}_1$ , one finds

$$\frac{dy}{dx} = -\frac{\lambda}{\sqrt{6}}. \quad (34)$$

Therefore, at late times, when the system evolves towards fixed point (11) the trajectory in the  $x$ - $y$  plane is

$$y \approx 1 - \frac{\lambda}{\sqrt{6}}x. \quad (35)$$

In figure 3 we plot the same models as shown in figure 1 and overlay this line. One can see that the trajectories indeed converge to this at late times once they have left the saddle point.

Finally, one can examine the behaviour of the determinant of the Jordan frame metric along this trajectory. We begin with the equations for the centre variables, where we have set  $A_1 = 0$ , which follows from the values of  $x$  and  $Y$  at the fixed point:

Name	$x$	$y$	$Z$	Existence
(8)	-1	0	1	All
(9)	0	0	1	All
(10)	1	0	1	All
(11)	0	1	1	All
(12)	$-\frac{\sqrt{2(\alpha-\gamma)^2-9}+\sqrt{2\alpha-\sqrt{2}\gamma}}{3\sqrt{3}}$	0	1	$\alpha - \gamma > \frac{3}{\sqrt{2}}$
(13)	$\frac{\sqrt{2(\alpha-\gamma)^2-9}-\sqrt{2\alpha+\sqrt{2}\gamma}}{3\sqrt{3}}$	0	1	$\alpha - \gamma > \frac{3}{\sqrt{2}}$
(14)	$\frac{\lambda}{\sqrt{6}}$	$\sqrt{1 - \frac{\lambda^2}{6}}$	1	$\lambda < \sqrt{6}$
(15)	$\frac{\sqrt{6}}{2\alpha-2\gamma+3\lambda}$	$\frac{\sqrt{\frac{6}{2\alpha-2\gamma+3\lambda}+2\alpha-2\gamma+\lambda}}{\sqrt{2\alpha-2\gamma+3\lambda}}$	1	$2\alpha - 2\gamma + 3\lambda > 0$
(16)	$\frac{\sqrt{4\gamma^2-6+2\gamma}}{\sqrt{6}}$	0	$\frac{1}{\sqrt{4\gamma^2-6+2\gamma+1}}$	$\gamma > \sqrt{\frac{2}{3}}$
(17)	$\frac{2\gamma-\sqrt{4\gamma^2-6}}{\sqrt{6}}$	0	$\frac{\sqrt{4\gamma^2-6+2\gamma+1}}{4\gamma+7}$	$\gamma > \sqrt{\frac{2}{3}}$

TABLE III. The fixed points of the compactified system system (24)–(26). Fixed points with  $Z = 0$  are not shown since they are already present in table I. Similarly, fixed points (4) and (5) are not shown. We have listed the condition for the existence of the fixed point but that is not to say that it lies inside the physical phase space; one should check with table IV to ensure that the cosmological parameters, especially  $\Omega_\phi$ , assume values inside the physical state space.

Name	$Q$	$\Omega_\phi$	$\omega_\phi$	$D$
(8)	$\pm\infty$	1	1	$\infty$
(9)	$\alpha$	0	0	$\infty$
(10)	$\pm\infty$	1	1	$\infty$
(12)	$\pm\infty$	$\frac{1}{27} \left( \sqrt{2(\alpha-\gamma)^2-9} + \sqrt{2\alpha-\sqrt{2}\gamma} \right)^2$	1	$\infty$
(13)	$\pm\infty$	$\frac{1}{27} \left( \sqrt{2(\alpha-\gamma)^2-9} + \sqrt{2\alpha-\sqrt{2}\gamma} \right)^2$	1	$\infty$
(14)	$\pm\infty$	1	$-1 + \lambda^2/3$	$\infty$
(15)	$\pm\infty$	$\frac{4\alpha^2-8\alpha\gamma+8\alpha\lambda+4\gamma^2-8\gamma\lambda+3\lambda^2+12}{(2\alpha-2\gamma+3\lambda)^2}$	$-\frac{(2\alpha-2\gamma+\lambda)(2\alpha-2\gamma+3\lambda)}{4\alpha^2-8\alpha\gamma+8\alpha\lambda+4\gamma^2-8\gamma\lambda+3\lambda^2+12}$	$\infty$
(16)	0	$\frac{1}{6} \left( \sqrt{4\gamma^2-6} + 2\gamma \right)^2$	1	1
(17)	0	$\frac{1}{6} \left( \sqrt{4\gamma^2-6} - 2\gamma \right)^2$	1	1

TABLE IV. The cosmological quantities at the fixed points of the compactified system. Note that  $Q \rightarrow \pm\infty$  reflects the fact that  $z \rightarrow \infty$ . The sign depends on the choice of  $\gamma$ ,  $\lambda$  and  $\alpha$ .

$$\frac{dA_2}{dN} = -\frac{3A_2(A_2+1)A_3(A_3(\lambda^2-6)+2\lambda(\lambda-2\gamma))}{2\lambda^2} \quad \text{and} \quad (36)$$

$$\begin{aligned} \frac{dA_3}{dN} = & -\frac{\lambda A_3 \left( \frac{6A_3}{\lambda^2} + A_3 + 2 \right) \left( (A_2+1) \left( 2\alpha + (A_2+1) \left( -\alpha + \frac{18A_3(2A_3(\alpha-\gamma)-\lambda)}{\lambda^2} - 3(A_3+1)^2\lambda \right) \right) - \alpha \right)}{2(A_2+1) \left( (A_2+1) \left( A_3^2 \left( \frac{54}{\lambda^2} + 3 \right) + 6A_3 - 1 \right) + 2 \right) - 2} \\ & - \frac{3A_3^2(A_3(\lambda^2-6)+2\lambda^2)}{2\lambda^2} - 3A_3 - \frac{(A_3+1)^2\lambda^2}{2}. \end{aligned} \quad (37)$$

One can then find the fixed points of this reduced phase space. The only two physical fixed points are

$$A_2 = \frac{12(\lambda-2\gamma)}{24\gamma \pm \lambda^2 - 12\lambda \pm 6} \quad \text{and} \quad A_3 = \frac{2\lambda(2\gamma-\lambda)}{\lambda^2-6}. \quad (38)$$

In these coordinates, one has

$$D = 1 - \frac{36A_3^2(A_2+1)^2}{\lambda^2 A_2^2} \quad (39)$$

and one can verify that this is indeed zero at these fixed points. Therefore, any trajectory in the  $x$ - $y$  plane that evolves towards this fixed point will evolve in such a way that  $\sqrt{-\tilde{g}} \rightarrow 0$  but only in the infinite future. This is the underlying reason for the pathology resistance discussed above: the system will evolve towards a metric singularity but only in the infinite future and therefore any trajectory must necessarily slow down as it is approached. To date, this feature has been observed nu-

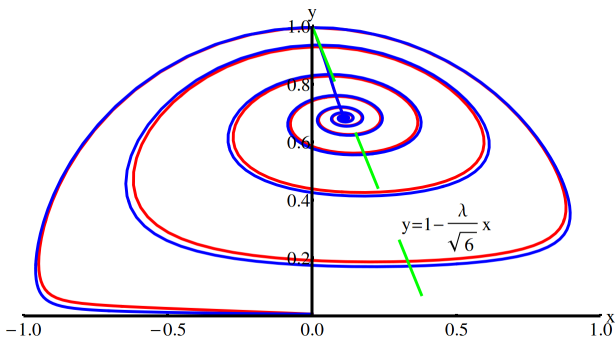


FIG. 3. The  $x$ - $y$  plane for the same models as figure 1 but overlaid with the centre manifold prediction for the late-time trajectories  $y = 1 - \lambda x/\sqrt{6}$  (green dashed line).

merically but no underlying reason has been discerned.

$$\frac{dx}{dN} = \sqrt{\frac{3}{2}} \frac{(x^2 + y^2 - 1) \left( x^2(2\alpha - \lambda) + \sqrt{6}x - y^2(\alpha\tilde{\Lambda}^2 + \lambda) \right)}{3x^2 - (\tilde{\Lambda}^2 - 1)y^2 - 1} + \frac{3}{2}x(x^2 - y^2 + 1) - 3x + \sqrt{\frac{3}{2}}\lambda y^2, \quad (40)$$

where the second equation is (15) and  $\tilde{\Lambda} \equiv \Lambda/m_0$ . The fixed points which lie inside the physical phase space are shown in table V and the cosmological quantities at these points are shown in table VI. Note that one has a choice of minimising either the  $x$ - $y$  or  $x$ - $z$  system. Either is fine, but it is important to note that the redundant equation acts as a constraint and should be identically zero at the fixed points. When this is not the case the points are unphysical and we do not include them. Points (18) and (19) are points (4) and (5), although they have different scalar charges and their stability is different; the interesting point is (20). We list the eigenvalues in appendix B. The stability of point (18) is identical to the conformal case but the stability of (19) is altered from both the conformal case and the case where  $\gamma \neq \lambda/2$ . Furthermore, one can check that point (20) is stable over a large range of parameter space and is often simultaneously stable when point (18) is. When point (18) does not exist, it is often the case that point (19) is unstable and (20) is the only stable attractor of the system.

Interestingly, this fixed point can match the current observations of dark energy and has  $Q = 0$  so that there are no fifth-forces in the solar system. To see this, consider as an example the WMAP9 results [31],  $\omega = -0.97$ ,  $\Omega_{DE} = 0.704$  [39]. One finds that fixed point (20) can reproduce this exactly by taking  $\lambda = 3.77953$  and  $\tilde{\Lambda} = 0.174519$  with  $\alpha$  arbitrary. As an example, consider the case  $\alpha = 2$ . In the purely conformal case the system would evolve to the variable fixed point where

What we have shown here is that this is a generic feature of models where the conformal fixed points are all unstable and furthermore, that the pathology resistance is present in any physical solution of the system.

#### IV. REDUCED PHASE SPACE

In this section, we examine the special parameter choice  $\gamma = \lambda/2$ , which we argued above reduces the dimension of the phase space to two and therefore requires a separate analysis. We can choose to eliminate either  $z$  or  $y$  from the equations and we choose to eliminate  $z$  in order to make contact with the purely conformal case. Furthermore,  $z \rightarrow \infty$  corresponds to  $y \rightarrow 0$  and so this substitution captures all of the new fixed points without having to compactify further. Using equation (18) in equations (14) and (15) we find the following two-dimensional autonomous system for  $x$  and  $y$ :

$\Omega_\phi \approx 0.436$  and  $\omega_\phi \approx -0.794$ , which are far from the WMAP values. In figure 4 we plot the  $x$ - $y$  plane for both the purely conformal case and the disformal case with the same initial conditions. One can see that the disformal trajectory converges to fixed point (20) whereas the purely conformal case reaches fixed point (18) (or rather, the conformal equivalent). To illustrate this further, we plot  $\Omega_\phi$  and  $\omega_\phi$  in figures 5 and 6. It is interesting to note that, unlike the purely conformal case where there is a lack of a matter dominated era [35], the disformal system delays the onset of the field rolling and allows for a period of matter domination. This behaviour was also noted in [18]. The screening of fifth-forces can be seen in figure 7, where we plot the local scalar charge. The purely conformal theory has  $Q = \alpha$  but  $Q \rightarrow 0$  for the disformal system as the fixed point is reached. Note that the bump at early times is due to the initial conditions. The field starts off with zero kinetic energy and begins to roll; a more realistic scenario including radiation would see the field rolling already. Such a system is beyond the scope of the present work. Finally, one can see that the fixed point has  $D = 1$ , and so there is a singularity of  $\sqrt{-\tilde{g}}$  in the infinite future. This is plotted in figure 8. This model then exhibits the natural pathology resistance discussed above since the singularity can only be reached in an infinite amount of time.



Name	$x$	$y$	Existence
(18)	$\frac{\lambda}{\sqrt{6}}$	$\sqrt{1 - \frac{\lambda^2}{6}}$	$\lambda < \sqrt{6}$
(19)	$\frac{\sqrt{\frac{3}{2}}}{\alpha + \lambda}$	$\frac{\sqrt{3 + 2\alpha(\alpha + \lambda)}}{\sqrt{2(\alpha + \lambda)}}$	$\alpha > 3/\lambda - \lambda$
(20)	$\frac{\lambda\tilde{\Lambda}^2 - \sqrt{(\lambda^2 - 6)\tilde{\Lambda}^4 + 12\tilde{\Lambda}^2}}{\sqrt{6(\tilde{\Lambda}^2 - 2)}}$	$\sqrt{6} \left( (\lambda^2 - 3)\tilde{\Lambda}^2 + \lambda\sqrt{\tilde{\Lambda}^2((\lambda^2 - 6)\tilde{\Lambda}^2 + 12)} + 6 \right)^{-1/2}$	$\lambda > \sqrt{3}$

TABLE V. The fixed points of the system when  $\gamma = \lambda/2$ . Note that the existence indicates where the point exists; one may find parameter choices where the point exists but lies outside the physical state space. Note that point (20) exists for all  $\tilde{\Lambda}$  when  $\lambda > \sqrt{3}$ . When the converse is true one can find a narrow region in the  $\tilde{\Lambda}$ - $\lambda$  plane where the point still exists. We will not be interested in this region in this work.

Name	$Q$	$\Omega_\phi$	$\omega_\phi$	$D$
(18)	$\frac{\alpha(\lambda^2(\tilde{\Lambda}^2 + 2) - 6\tilde{\Lambda}^2)}{(\lambda^2 - 6)\tilde{\Lambda}^2}$	1	$-1 + \frac{\lambda^2}{3}$	$-\frac{2\lambda^2}{(\lambda^2 - 6)\tilde{\Lambda}^2}$
(19)	$\alpha - \frac{6}{\tilde{\Lambda}^2(2\alpha^2 + 2\alpha\lambda + 3)}$	$\frac{\alpha(\alpha + \lambda) + 3}{(\alpha + \lambda)^2}$	$-1 + \frac{3}{3 + \alpha(\alpha + \lambda)}$	$\frac{6}{\tilde{\Lambda}^2(2\alpha(\alpha + \lambda) + 3)}$
(20)	0	$\frac{3(\tilde{\Lambda}^2 + 2)}{(\lambda^2 - 3)\tilde{\Lambda}^2 + \lambda\sqrt{(\lambda^2 - 6)\tilde{\Lambda}^4 + 12\tilde{\Lambda}^2} + 6}$	$1 - \frac{4}{\tilde{\Lambda}^2 + 2}$	1

TABLE VI. The cosmological quantities at the fixed points of the system when  $\gamma = \lambda/2$ .

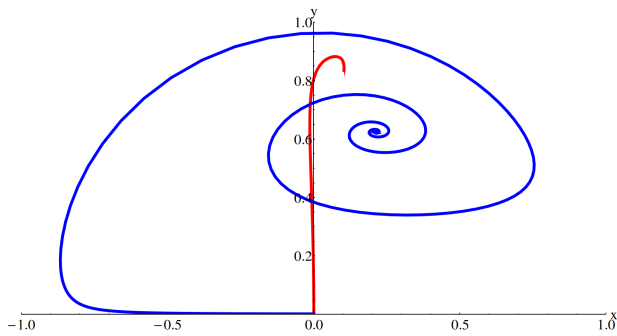


FIG. 4. The trajectories in the  $x$ - $y$  plane for a purely conformal theory with  $\alpha = 2$  (blue) and a disformal theory with  $\gamma = \lambda/2$  (red). In each case the initial conditions are  $\phi_0 = -1$  and  $\phi'_0 = 0$ . The parameters  $\Lambda$ ,  $m_0$  and  $\lambda$  were chosen such that the disformal attractor corresponds to a universe where  $\omega_\phi$  and  $\Omega_\phi$  match the WMAP9 observations.

## V. CONCLUSIONS

In this work we have studied the solution space of disformal theories of gravity using dynamical systems techniques. Our ultimate goal was to find stable dark energy dominated solutions where the local scalar charge is zero at late times.

We argued that, in the general case, the phase space of the system is three-dimensional rather than the two-dimensional phase space of the equivalent quintessence and purely conformal theories. It was found that there are no new interesting fixed points of the system and furthermore there are parameter choices where the attractors that are reached in the purely conformal case are now saddle points. This is due to the increased dimension of the phase space, which changes the characteristic

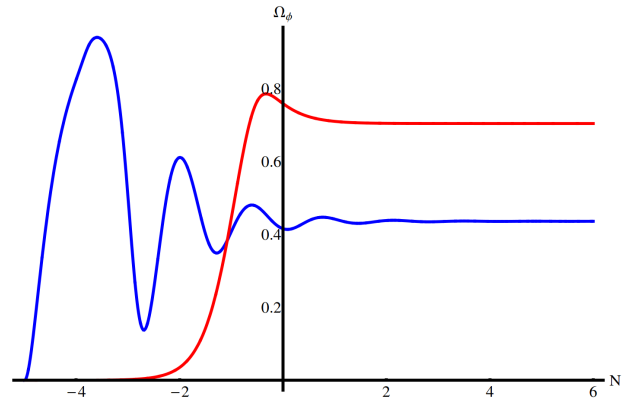


FIG. 5.  $\Omega_\phi$  as a function of  $N$  for a purely conformal theory with  $\alpha = 2$  (blue) and a disformal theory with  $\gamma = \lambda/2$  (red). The parameters and initial conditions are as indicated in figure 4's caption.

polynomial for the eigenvalues to a cubic equation rather than a quadratic, yielding a third solution that can be positive. Numerically, we observed that when the parameters assume these values, the trajectories spend a long time near this saddle point before evolving towards a dark energy dominated fixed point with infinite local scalar charge. Two of the eigenvalues at this fixed point are zero and so it was necessary to use centre manifold techniques to discern the late-time behaviour.

The Jordan frame metric can become singular, indicating a potential instability of the theory. Several previous works have noted a natural resistance to pathology where numerical solutions show that the field slows down as the singularity is approached. Here, we were able to explain this by showing that any singularity is only reached in an infinite amount of time.

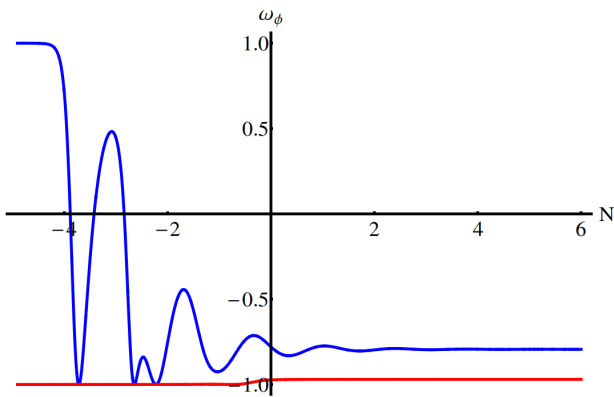


FIG. 6.  $\omega_\phi$  as a function of  $N$  for a purely conformal theory with  $\alpha = 2$  (blue) and a disformal theory with  $\gamma = \lambda/2$  (red). The parameters and initial conditions are as indicated in figure 4's caption.

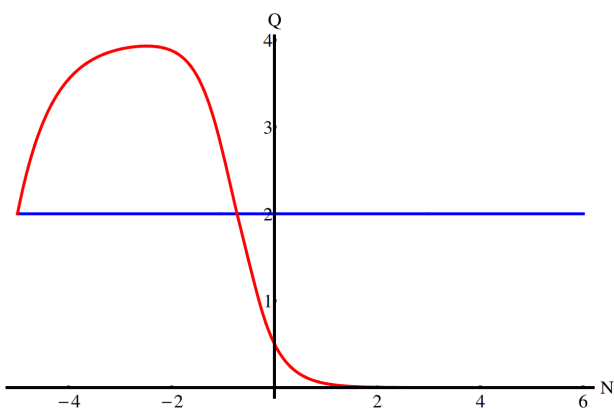


FIG. 7. The local scalar charge as a function of  $N$  for a purely conformal theory with  $\alpha = 2$  (blue) and a disformal theory with  $\gamma = \lambda/2$  (red). The parameters and initial conditions are as indicated in figure 4's caption.

We identified a tuning in parameter space,  $\gamma = \lambda/2$ , where the dimension of the phase space is reduced to two and therefore the dynamics are very different. There is a fixed point—point (20)—of the reduced phase space not present in the purely conformal system. This point is a stable attractor and produces a viable scenario: the local scalar charge is identically zero so that there are no fifth-forces in the solar system and one can find parameter values such that the dark energy parameters match the observed values. In particular, by taking  $\lambda = 3.77953$  and  $\tilde{\Lambda} = 0.174519$  we were able to reproduce the WMAP9 density parameter and equation of state.

It seems that this fixed point is a good candidate for future study but there are still many important questions to answer. Here we have taken the simplest model where  $\gamma$ ,  $\lambda$  and  $\alpha$  are constants. When they are allowed to vary, the dynamics are altered and one must think of the points

found here as instantaneous fixed points. One can then investigate the dynamics of the new system, which may

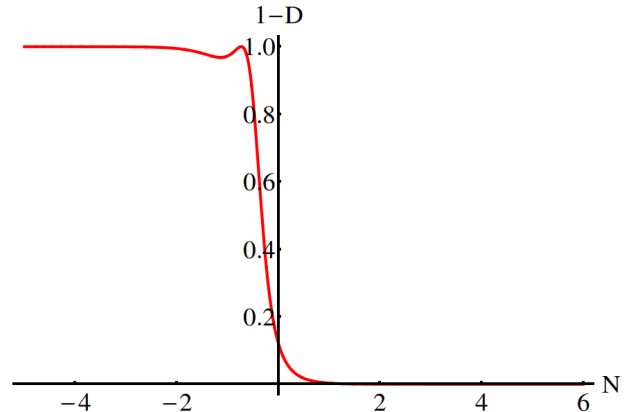


FIG. 8.  $(1 - D)$  as a function of  $N$  for the disformal system that approaches fixed point (20). The parameters and initial conditions are as indicated in figure 4's caption.

have a dimension larger than three, or try to find models where the late-time fixed points give the observed dark energy parameters. In terms of our model, the choice  $\gamma = \lambda/2$  was a parameter tuning but for more general models one requires that  $\gamma(\phi) = \lambda(\phi)/2$  is reached dynamically. It remains to be seen if one can contrive more general models where this is achieved. One may also worry that quantum corrections can spoil this tuning; this certainly merits investigation.

Only recently have the properties of disformal theories been fully elucidated and, unlike more well-studied models, there is no canonical disformal paradigm. Indeed, to date, a viable model that screens fifth-forces and can account for all cosmological observations is still lacking. What we have done here is to classify the possible cosmological solutions and identify a class of models—albeit using a special tuning—that can reproduce the observed dark energy parameters today and satisfy local tests of gravity. Future studies must assess how well these models can fit probes of the expansion history such as the supernova luminosity distance as well as linear probes such as the CMB. It would also be interesting to study the cosmology of more realistic models that include components neglected here such as radiation.

## ACKNOWLEDGEMENTS

I am incredibly grateful to Claes Uggla for several enlightening conversations and for bringing new techniques such as the centre manifold to my attention. Research at Perimeter Institute is supported by the Government of Canada through Industry Canada and by the Province of Ontario through the Ministry of Economic Development & Innovation.

- 
- [1] A. G. Riess *et al.* (Supernova Search Team), *Astron.J.* **116**, 1009 (1998), arXiv:astro-ph/9805201 [astro-ph].
- [2] S. Perlmutter *et al.* (Supernova Cosmology Project), *Astrophys.J.* **517**, 565 (1999), arXiv:astro-ph/9812133 [astro-ph].
- [3] T. Clifton, P. G. Ferreira, A. Padilla, and C. Skordis, *Phys.Rept.* **513**, 1 (2012), arXiv:1106.2476 [astro-ph.CO].
- [4] A. Joyce, B. Jain, J. Khoury, and M. Trodden, (2014), arXiv:1407.0059 [astro-ph.CO].
- [5] J. Khoury and A. Weltman, *Phys.Rev.Lett.* **93**, 171104 (2004), arXiv:astro-ph/0309300 [astro-ph].
- [6] J. Khoury and A. Weltman, *Phys. Rev.* **D69**, 044026 (2004), arXiv:astro-ph/0309411.
- [7] K. Hinterbichler, J. Khoury, A. Levy, and A. Matas, (2011), arXiv:1107.2112 [astro-ph.CO].
- [8] P. Brax, C. van de Bruck, A.-C. Davis, and D. Shaw, *Phys. Rev.* **D82**, 063519 (2010), arXiv:1005.3735 [astro-ph.CO].
- [9] A. Vainshtein, *Phys.Lett.* **B39**, 393 (1972).
- [10] Note that some theories such as massive gravity [40] utilise these mechanisms, although the coupling to matter is only seen explicitly in the decoupling limit.
- [11] J. D. Bekenstein, in *Marcel Grossmann Meeting on General Relativity*, edited by F. Satō and T. Nakamura (1992) p. 905.
- [12] J. D. Bekenstein, *Phys.Rev.* **D48**, 3641 (1993), arXiv:gr-qc/9211017 [gr-qc].
- [13] T. S. Koivisto, (2008), arXiv:0811.1957 [astro-ph].
- [14] M. Zumalacarregui, T. Koivisto, D. Mota, and P. Ruiz-Lapuente, *JCAP* **1005**, 038 (2010), arXiv:1004.2684 [astro-ph.CO].
- [15] J. Noller, *JCAP* **1207**, 013 (2012), arXiv:1203.6639 [gr-qc].
- [16] M. Zumalacarregui, T. S. Koivisto, and D. F. Mota, *Phys.Rev.* **D87**, 083010 (2013), arXiv:1210.8016 [astro-ph.CO].
- [17] M. Zumalacarregui and J. Garca-Bellido, *Phys.Rev.* **D89**, 064046 (2014), arXiv:1308.4685 [gr-qc].
- [18] J. Sakstein, (2014), arXiv:1409.1734 [astro-ph.CO].
- [19] A.-C. Davis, E. A. Lim, J. Sakstein, and D. Shaw, *Phys.Rev.* **D85**, 123006 (2012), arXiv:1102.5278 [astro-ph.CO].
- [20] B. Jain, V. Vikram, and J. Sakstein, *Astrophys.J.* **779**, 39 (2013), arXiv:1204.6044 [astro-ph.CO].
- [21] P. Brax, A.-C. Davis, and J. Sakstein, (2013), arXiv:1301.5587 [gr-qc].
- [22] J. Sakstein, *Phys.Rev.* **D88**, 124013 (2013), arXiv:1309.0495 [astro-ph.CO].
- [23] V. Vikram, J. Sakstein, C. Davis, and A. Neil, (2014), arXiv:1407.6044 [astro-ph.CO].
- [24] J. Sakstein, B. Jain, and V. Vikram, (2014), 10.1142/S0218271814420024, arXiv:1409.3708 [astro-ph.CO].
- [25] P. C. Freire, N. Wex, G. Esposito-Farese, J. P. Verbiest, M. Bailes, *et al.*, *Mon.Not.Roy.Astron.Soc.* **423**, 3328 (2012), arXiv:1205.1450 [astro-ph.GA].
- [26] J. Khoury, (2014), arXiv:1409.0012 [hep-th].
- [27] One could screen this using the Damour-Polyakov effect [41], although this has not yet been investigated.
- [28] E. J. Copeland, A. R. Liddle, and D. Wands, *Phys.Rev.* **D57**, 4686 (1998), arXiv:gr-qc/9711068 [gr-qc].
- [29] B. Gumjudpai, T. Naskar, M. Sami, and S. Tsujikawa, *JCAP* **0506**, 007 (2005), arXiv:hep-th/0502191 [hep-th].
- [30] E. J. Copeland, M. Sami, and S. Tsujikawa, *Int.J.Mod.Phys.* **D15**, 1753 (2006), arXiv:hep-th/0603057 [hep-th].
- [31] G. Hinshaw *et al.* (WMAP), *Astrophys.J.Suppl.* **208**, 19 (2013), arXiv:1212.5226 [astro-ph.CO].
- [32] Note that we are using the conventions of [18]. A dictionary to convert these conventions to others in the literature such as [16] can be found there.
- [33] Note that this was studied briefly in [16], appendix C.
- [34] The parameter space is spanned by  $\gamma$ ,  $\alpha$ ,  $\lambda$  and  $\Lambda/m_0$ .
- [35] L. Amendola, *Phys.Rev.* **D62**, 043511 (2000), arXiv:astro-ph/9908023 [astro-ph].
- [36] Note that  $z = 0$  does not necessarily mean that  $B = 0$ . Since  $z \propto H$  these points may correspond to the infinite future where  $H = 0$ .
- [37] We have not included fixed points where  $Z > 1$  or  $Z < 0$ , which lie outside the physical state space. Furthermore, one finds that there is an additional fixed point when  $\gamma \rightarrow \infty$  where  $Z = 1$ , which we also ignore. This may be relevant for models where  $\gamma$  can reach infinity.
- [38] A. Alho and C. Ugglä, (2014), arXiv:1406.0438 [gr-qc].
- [39] Note that this data set assumes that  $\omega$  is fixed whereas it varies in our model and so a more realistic method would to use a varying  $\omega$  fit such as the  $\omega_0 - \omega_a$  parametrisation. The analysis here is a proof of principle only and so we will not concern ourselves with a more realistic data analysis.
- [40] C. de Rham, G. Gabadadze, and A. J. Tolley, *Phys.Rev.Lett.* **106**, 231101 (2011), arXiv:1011.1232 [hep-th].
- [41] T. Damour and A. M. Polyakov, *Nucl. Phys.* **B423**, 532 (1994), arXiv:hep-th/9401069.
- [42] We are interested in stable fixed points since these describe the late-time behaviour of the system and so we will not consider positive eigenvalues here.

## Appendix A: Dynamical Systems

In this section we briefly review the aspects of dynamical systems theory required to study the disformal system.

### 1. Fixed Points and Stability

Consider a system described by  $n$  first-order ordinary differential equations for  $n$  variables  $X_i$  as a function of some “time” coordinate  $t$  and let a dot denote derivatives with respect to this. If the system can be written in the form

$$\frac{dX_i}{dt} = f_i(\{X_j\}), \quad (\text{A1})$$

then it is known as an *autonomous* system and one can use dynamical systems techniques to classify the solutions. The phase space of the system is the  $n$ -dimensional space spanned by  $\{X_j\}$  and solutions of the system correspond to trajectories in this space. A fixed point of the system is one where  $\dot{f}_i = 0 \forall i$ . This is a set of  $n$  algebraic equations that can be solved for the values of the fixed points  $\{X_j^c\}$ . If one tunes the variables to  $\{X_j^c\}$  then the system will not evolve but one is generally interested in the behaviour of arbitrary trajectories. In particular, if the fixed points are such that trajectories flow towards them at late times then the final state of the system is known independently of the initial conditions and so one can make important inferences about the late-time behaviour of all solutions. In this case, the point is known as an *attractor*. If the trajectories flow away from the fixed point it is known as a *repellor*. Finding and classifying all of the fixed points of a system is tantamount to understanding the behaviour of all possible solutions, which is especially important if one lacks analytic solutions. Cosmologically, one can calculate several important quantities such as the density parameter and the equation of state and so dynamical systems techniques have become an important tool to assess the viability of dark energy models.

One may determine the stability of the fixed points as follows. Consider linearising the system about a fixed point such that  $X_i = X_i^c + \delta X_i$ .  $\delta X_i$  satisfies the equation

$$\delta \dot{X}_i = M_{ij} \delta X_j \quad (\text{A2})$$

where

$$M_{ij} = \frac{\partial f_i}{\partial X_j}, \quad (\text{A3})$$

and we have ignored second order contributions since  $\delta X_i$  is a small perturbation. This means that the stability analysis holds for regions of phase space close enough to the fixed points such that this linearisation is a good approximation. Changing to the eigenbasis  $\vec{e}_i$  of  $M$  one has ( $A_j$  are new variables parametrising the system in the eigenbasis)

$$X_i = \sum_j A_j (\vec{e}_j)_i \quad (\text{A4})$$

so that the equation for  $\delta A_j$  is

$$\delta \dot{A}_j = e_j \delta A_j, \quad (\text{A5})$$

where  $e_j$  is the eigenvalue associated with  $\vec{e}_j$ . One then has  $\delta A_j \sim e^{e_j t}$  and so the stability of the fixed point in the direction  $\vec{e}_j$  is determined by  $e_j$ . There are several possibilities:

- $e_j$  is real and  $e_j > 0 \forall j$ : Trajectories in the direction flow away from the fixed point and it is known as an *unstable node*.

- $e_j$  is real and  $e_j < 0 \forall j$ : Trajectories in the direction flow towards the fixed point and it is known as a *stable node*.
- $e_j$  is complex and  $\Re e_j > 0 \forall j$ : Trajectories spiral away from the fixed point. In this case the point is known as an *unstable spiral*.
- $e_j$  is complex and  $\Re e_j < 0 \forall j$ : Trajectories spiral towards the fixed point; the point is known as a *stable spiral* in this case.
- There are a mixture of eigenvalues with differing signs for  $\Re e_j$ . In this case there are some stable directions and some unstable directions and the fixed point is known as a *saddle point*.

At late times, trajectories in phase space flow away from unstable nodes and towards stable nodes. The system may spend prolonged periods of time near saddle points but will ultimately evolve towards a stable node. We have not discussed the case where the system contains one or more zero eigenvalues. The simplest cosmological systems all have non-zero eigenvalues but, as we have seen above, disformal theories contain a fixed point with two zero directions and so here we must use more advanced techniques. This is the subject of the next subsection.

## 2. Centre Manifolds

The centre manifold technique is used when the fixed point has one or more zero eigenvalues. Here we give a brief introduction and include only those aspects of the technique relevant for the problems studied in the main text.

Let us consider a fixed point described by  $n-p$  negative (or negative real part) eigenvalues with corresponding eigenvectors  $\vec{E}_j$  and  $p$  zero eigenvalues with eigenvectors  $\vec{e}_j$  [42]. One may expand the variables in terms of the eigenbasis such that

$$X_i = \sum_{j=1}^{n-p} A_j^s (\vec{E}_j)_i + \sum_{j=n-p+1}^n A_j^c (\vec{e}_j)_i, \quad (\text{A6})$$

where we label stable directions as  $A_j^s$  and zero eigenvalue or *centre* directions as  $A_j^c$ . The zero eigenvalues indicate that a linear analysis is not sufficient to analyse the stability in the directions of  $\vec{e}_j$ . This is a problem with two time scales. Trajectories in the directions of  $\vec{E}_j$  will converge to the attractor swiftly but the behaviour of the components in the directions of  $\vec{e}_j$  is unknown. The centre manifold technique allows one to solve for the late-time behaviour of  $A_j^c$  by working on time scales such that  $A_j^s$  have converged to their trajectories along the attractor. One then reduces the dimension of the phase space from  $n$  to  $p$  and can formulate the system as an autonomous one in the hope of being able to derive

the behaviour of  $A_j^c$ . This works as follows: the full  $n$ -dimensional system can be described by the autonomous system

$$\frac{dA_i^s}{dt} = g_i(\vec{A}^s, \vec{A}^c) \quad i = 1, \dots, n-p \quad \text{and} \quad (\text{A7})$$

$$\frac{dA_i^c}{dt} = h_i(\vec{A}^s, \vec{A}^c) \quad i = n-p+1, \dots, n. \quad (\text{A8})$$

Setting,  $g_i = 0$  gives  $n-p$  algebraic equations, which allows one to solve for  $\vec{A}^s(\vec{A}^c)$  along trajectories at sufficiently late times such that the attractor has been reached in the  $\vec{E}_j$  directions. The dynamics in the reduced,  $p$ -dimensional phase space are then described by

$$\frac{dA_i^c}{dt} = h_i(\vec{A}^s(\vec{A}^c), \vec{A}^c) \quad i = n-p+1, \dots, n. \quad (\text{A9})$$

This represents a new Autonomous system that can be investigated using the techniques of section A 1 to discern the late-time behaviour.

## Appendix B: Eigenvalues at the Fixed Points

In this appendix we list the eigenvalues for each fixed point. Points (18)–(20) are those of the two-dimensional phase space when  $\gamma = \lambda/2$  and so there are only two eigenvalues.

### 1. Eigenvalues

- 
- (1)  $e_1 = 3 - \sqrt{6}\alpha$ ,  $e_2 = -\sqrt{6}\gamma - 3$ ,  $e_3 = \sqrt{3/2}\lambda + 3$
  - (2)  $e_1 = \sqrt{6}\alpha + 3$ ,  $e_2 = \sqrt{6}\gamma - 3$ ,  $e_3 = 3 - \sqrt{3/2}\lambda$
  - (3)  $e_1 = \alpha^2 - 3/2$ ,  $e_2 = -\alpha(\alpha + 2\gamma) - 3/2$ ,  $e_3 = \alpha(\alpha + \lambda) + 3/2$
  - (4)  $e_1 = \lambda(\gamma - \lambda/2)$ ,  $1/2(\lambda^2 - 6)$ ,  $e_3 = \lambda(\alpha + \lambda) - 3$
  - (5)  $e_1 = 3(2\gamma - \lambda)/2(\alpha + \lambda)$ ,  $e_2 = (6\alpha + 3\lambda - \sqrt{-3(32\alpha^2 + 21)\lambda^2 + 12\alpha(9 - 4\alpha^2)\lambda + 36(5\alpha^2 + 6) - 48\alpha\lambda^3})/4(\alpha + \lambda)$ ,  
 $e_3 = (\sqrt{12\alpha(9 - 4\alpha^2)\lambda - 3(32\alpha^2 + 21)\lambda^2 + 36(5\alpha^2 + 6) - 48\alpha\lambda^3} - 6\alpha - 3\lambda)/4(\alpha + \lambda)$
  - (6)  $e_1 = \frac{3(2\gamma - \lambda)}{2(\alpha + \lambda)}$ ,  $e_2 = 3/2 \sqrt{\frac{8\alpha^2 - 4\alpha(\sqrt{4\gamma^2 - 6} - 4\gamma) + 10\gamma^2 - 4\gamma\sqrt{4\gamma^2 - 6} - 3}{2\gamma(\sqrt{4\gamma^2 - 6} + 2\gamma) - 3}} - 9/2 - 3/2(\sqrt{4\gamma^2 - 6} - 2\gamma)(2\alpha + 5\gamma)$ ,  
 $e_3 = -3/2(\sqrt{4\gamma^2 - 6} - 2\gamma)(2\alpha + 5\gamma) - 3/2 \sqrt{\frac{8\alpha^2 - 4\alpha(\sqrt{4\gamma^2 - 6} - 4\gamma) + 10\gamma^2 - 4\gamma\sqrt{4\gamma^2 - 6} - 3}{2\gamma(\sqrt{4\gamma^2 - 6} + 2\gamma) - 3}} + 9/2$
  - (7)  $e_1 = 1/2(\sqrt{4\gamma^2 - 6} + 2\gamma)(2\gamma - \lambda)$ ,  $e_2 = \frac{3((\sqrt{4\gamma^2 - 6} - 2\gamma)(2\alpha - \gamma) + U_1 - 9)}{4\gamma(\sqrt{4\gamma^2 - 6} - 2\gamma) + 6}$ ,  $e_3 = \frac{3((\sqrt{4\gamma^2 - 6} - 2\gamma)(2\alpha - \gamma) - U_1 - 9)}{4\gamma(\sqrt{4\gamma^2 - 6} - 2\gamma) + 6}$
  - (8)  $e_1 = \sqrt{6}\gamma + 3$ ,  $e_2 = -\sqrt{6}\alpha + \sqrt{6}\gamma + 6$ ,  $e_3 = \sqrt{\frac{3}{2}}\lambda + 3$
  - (9)  $e_1 = 3/2$ ,  $e_2 = 3/2$ ,  $e_3 = 3/2$
  - (10)  $e_1 = 3 - \sqrt{6}\gamma$ ,  $e_2 = \sqrt{6}\alpha - \sqrt{6}\gamma + 6$ ,  $e_3 = 3 - \sqrt{\frac{3}{2}}\lambda$
  - (11)  $e_1 = -3$ ,  $e_2 = 0$ ,  $e_3 = 0$
  - (12)  $e_1 = \frac{1}{9}\left(\left(\sqrt{4(\alpha - \gamma)^2 - 18} + 2\alpha - 2\gamma\right)(\alpha - \gamma) - 18\right)$ ,  $e_2 = \frac{1}{9}\left((\alpha + 2\gamma)\left(\sqrt{4(\alpha - \gamma)^2 - 18} + 2\alpha - 2\gamma\right) + 9\right)$ ,  
 $e_3 = \frac{1}{18}\left(\left(\sqrt{4(\alpha - \gamma)^2 - 18} + 2\alpha - 2\gamma\right)(2\alpha - 2\gamma + 3\lambda) + 18\right)$
  - (13)  $e_1 = \frac{1}{9}\left(\left(-\sqrt{4(\alpha - \gamma)^2 - 18} + 2\alpha - 2\gamma\right)(\alpha - \gamma) - 18\right)$ ,  $e_2 = \frac{1}{9}\left(9 - (\alpha + 2\gamma)\left(\sqrt{4(\alpha - \gamma)^2 - 18} - 2\alpha + 2\gamma\right)\right)$ ,  
 $e_3 = \frac{1}{18}\left(18 - \left(\sqrt{4(\alpha - \gamma)^2 - 18} - 2\alpha + 2\gamma\right)(2\alpha - 2\gamma + 3\lambda)\right)$
  - (14)  $e_1 = \frac{1}{2}\lambda(\lambda - 2\gamma)$ ,  $e_2 = \frac{1}{2}(\lambda^2 - 6)$ ,  $e_3 = \alpha\lambda - \gamma\lambda + \frac{3\lambda^2}{2} - 3$
  - (15)  $e_1 = \frac{3\lambda - 6\gamma}{2\alpha - 2\gamma + 3\lambda}$ ,  
 $e_2 = -\frac{3(U_2 + (\alpha - \gamma + \lambda)(\lambda(2\alpha - 2\gamma + 3\lambda) - 12)(2\alpha - 2\gamma + 3\lambda)^{5/2})}{(2\alpha - 2\gamma + 3\lambda)^{7/2}(\lambda(2\alpha - 2\gamma + 3\lambda) - 12)}$ ,  $e_3 = \frac{3(U_2 - (\alpha - \gamma + \lambda)(2\alpha - 2\gamma + 3\lambda)^{5/2}(\lambda(2\alpha - 2\gamma + 3\lambda) - 12))}{(2\alpha - 2\gamma + 3\lambda)^{7/2}(\lambda(2\alpha - 2\gamma + 3\lambda) - 12)}$

$$\begin{aligned}
(16) \quad e_1 &= \frac{1}{2} \left( \sqrt{4\gamma^2 - 6} + 2\gamma \right) (2\gamma - \lambda), \\
e_2 &= \frac{1}{2} \left( \left( \sqrt{4\gamma^2 - 6} + 2\gamma \right) (2\alpha + 5\gamma) + U_3 - 9 \right), \quad e_3 = \frac{1}{2} \left( \left( \sqrt{4\gamma^2 - 6} + 2\gamma \right) (2\alpha + 5\gamma) - U_3 - 9 \right) \\
(17) \quad e_1 &= -\frac{1}{2} \left( \sqrt{4\gamma^2 - 6} - 2\gamma \right) (2\gamma - \lambda), \\
e_2 &= \frac{1}{2} \left( \left( \sqrt{4\gamma^2 - 6} + 2\gamma \right) (2\alpha + 5\gamma) + U_3 - 9 \right), \quad e_3 = \frac{1}{2} \left( \left( \sqrt{4\gamma^2 - 6} + 2\gamma \right) (2\alpha + 5\gamma) - U_3 - 9 \right) \\
(18) \quad e_1 &= \frac{1}{2} (\lambda^2 - 6), \quad e_2 = \lambda(\alpha + \lambda) - 3 \\
(19) \quad e_1 &= -\frac{6(2\alpha^2\lambda + 3\alpha(\lambda^2 - 4) + \lambda^3) + \sqrt{3}U_4 + 3\tilde{\Lambda}^2(2\alpha + \lambda)(2\alpha(\alpha + \lambda) + 3) - 36\lambda}{4(\alpha + \lambda)(2(\alpha + \lambda)(\alpha\tilde{\Lambda}^2 + \lambda) + 3(\tilde{\Lambda}^2 - 4))}, \\
e_2 &= \frac{-6(2\alpha^2\lambda + 3\alpha(\lambda^2 - 4) + \lambda^3) + \sqrt{3}U_4 - 3\tilde{\Lambda}^2(2\alpha + \lambda)(2\alpha(\alpha + \lambda) + 3) + 36\lambda}{4(\alpha + \lambda)(2(\alpha + \lambda)(\alpha\tilde{\Lambda}^2 + \lambda) + 3(\tilde{\Lambda}^2 - 4))} \\
(20) \quad e_1 &= \frac{(\Lambda^2 - 2)(\Lambda^2(4\alpha\lambda + 5\lambda^2 - 18) - \Lambda(4\alpha + 5\lambda)\sqrt{(\lambda^2 - 6)\Lambda^2 + 12 + 36}) - \sqrt{2}U_5}{4(\Lambda^2 - 2)}, \\
e_2 &= \frac{(\Lambda^2 - 2)(\Lambda^2(4\alpha\lambda + 5\lambda^2 - 18) - \Lambda(4\alpha + 5\lambda)\sqrt{(\lambda^2 - 6)\Lambda^2 + 12 + 36}) + \sqrt{2}U_5}{4(\Lambda^2 - 2)}
\end{aligned}$$

where

$$\begin{aligned}
U_1^2 &= 9 - 8\alpha^2 \left( 2\gamma \left( \sqrt{4\gamma^2 - 6} - 2\gamma \right) + 3 \right) - 4\alpha \left( 4 \left( \sqrt{4\gamma^2 - 6} - 2\gamma \right) \gamma^2 + 3\sqrt{4\gamma^2 - 6} \right) \\
&\quad + 8\gamma^4 + 6\gamma^2 - 6\sqrt{4\gamma^2 - 6}\gamma - 4\sqrt{4\gamma^2 - 6}\gamma^3, \tag{B1}
\end{aligned}$$

$$\begin{aligned}
U_2^2 &= (2\alpha - 2\gamma + 3\lambda)^5 (38\lambda^3(\alpha - \gamma) + \lambda^2(35(\alpha - \gamma)^2 - 12) + 10\lambda((\alpha - \gamma)^2 - 6)(\alpha - \gamma) \\
&\quad - 36((\alpha - \gamma)^2 + 1) + 12\lambda^4)(\lambda(2\alpha - 2\gamma + 3\lambda) - 12), \tag{B2}
\end{aligned}$$

$$\begin{aligned}
U_3^2 &= \left( \left( \sqrt{4\gamma^2 - 6} + 2\gamma \right) (2\alpha + 5\gamma) - 9 \right)^2 - 8 \left( \alpha \left( 4\gamma \left( \sqrt{4\gamma^2 - 6} + 2\gamma \right) - 3 \right) - 3\sqrt{4\gamma^2 - 6} \right) \\
&\quad + \gamma \left( 2\gamma \left( 4\gamma \left( \sqrt{4\gamma^2 - 6} + 2\gamma \right) - 15 \right) - 9\sqrt{4\gamma^2 - 6} \right) + 9, \tag{B3}
\end{aligned}$$

$$\begin{aligned}
U_4^2 &= - \left( \tilde{\Lambda}^2(2\alpha(\alpha + \lambda) + 3) (16\alpha^3\lambda + 4\alpha^2(8\lambda^2 - 15) + 4\alpha\lambda(4\lambda^2 - 9) + 21\lambda^2 - 72) \right. \\
&\quad \left. - 6(20\alpha^3\lambda + 8\alpha^2(5\lambda^2 - 9) + 3\alpha(7\lambda^2 - 16)\lambda + \lambda^4 + 18\lambda^2 - 72) \right) \left( 2(\alpha + \lambda)(\alpha\tilde{\Lambda}^2 + \lambda) + 3(\tilde{\Lambda}^2 - 4) \right) \quad \text{and} \tag{B4}
\end{aligned}$$

$$\begin{aligned}
U_5^2 &= \Lambda^4((4\alpha + 3\lambda)(4\alpha(\lambda^2 - 3) + 3\lambda(\lambda^2 - 5)) + 18) - 12\Lambda(4\alpha + 3\lambda)\sqrt{(\lambda^2 - 6)\Lambda^2 + 12} \\
&\quad - \Lambda^3(4\alpha + 3\lambda)(4\alpha\lambda + 3\lambda^2 - 6)\sqrt{(\lambda^2 - 6)\Lambda^2 + 12} + 6\Lambda^2((4\alpha + 3\lambda)(4\alpha + 5\lambda) - 12) + 72. \tag{B5}
\end{aligned}$$

### Appendix C: The $x$ - $Y$ - $W$ System

Here, we present the autonomous system written using the variables  $Y$  and  $W$  defined in (28) and (29):

$$\begin{aligned}
\frac{dx}{dN} &= \frac{\sqrt{6}(x^2 + Y(Y + 2))((W + 1)(2\alpha + (W + 1)(-\alpha + 3x(2x(\alpha - \gamma) + \sqrt{6}) - 3\lambda(Y + 1)^2)) - \alpha)}{2(W + 1)((W + 1)(9x^2 + 3(Y + 1)^2 - 4) + 2) - 2} \\
&\quad + \frac{3}{2}x(x^2 - Y(Y + 2)) - 3x + \sqrt{6}\lambda(Y + 1)^2, \tag{C1}
\end{aligned}$$

$$\frac{dY}{dN} = -\frac{1}{2}(Y + 1)(-3x^2 + \sqrt{6}\lambda x + 3Y(Y + 2)) \quad \text{and} \tag{C2}$$

$$\frac{dW}{dN} = \frac{1}{2}W(W + 1)(3x^2 - 2\sqrt{6}\gamma x - 3Y(Y + 2)). \tag{C3}$$